MICHIGAN STATE UNIVERSITY

CYCLOTRON LABORATORY

NEW VISTAS IN THE NUCLEAR SHELL MODEL

Invited talk given at the Symposium in Honor of Akito Arima:
Nuclear Physics in the 1990's, Santa Fe, May 1-5, 1990

B. ALEX BROWN

JULY 1990

MSUCL-733

MSUCL-733
July, 1990

NEW VISTAS IN THE NUCLEAR SHELL MODEL

B. Alex BROWN

National Superconducting Cyclotron Laboratory and Department of Physics and Astronomy, Michigan State University, E. Lansing, Mi, 48824, USA.

The general problems and gals of modern shell-model calculations are briefly reviewed. They are illustrated by the application to three questions current interest. (1) How is the a"gular momentum in a nucleus distributed between the orbital and the intrinsic spin degrees of freedom? (2) What are the orbital occupations and spacial extent of the neutrons in nuclei near the neutron drip line? and (3) Can we understand two-neutrino double beta decay in nuclei?

1. INTRODUCTION

It is a great pleasure for me to speak at this meeting in honor of Akito Arima, which is intended to look forward to the nuclear physics of the 1990's. Akito introduced me to the nuclear shell model at Stony Brook in the early 1970's, and my JSPS (Japan Society for the Promotion of Science) fellowship in 1974 enabled me to spend my first post-graduate year in the Arima-ken at the University of Tokyo. This was a very valuable experience for me both in physics and culture. I have always appreciated Akito's broad-ranging contributions to nuclear theory and his emphasis on phenomenology.

The nuclear shell model has bee" extensively developed over the past 40 years [1,2]. The great simplifying feature of the shell model approach is that there are bunchings of the orbits in the single-particle potential which results in a few doubly closed-shell nuclear ground states, some regions of deformed ground and excited states, and some regions of superdeformed excited states which can all be treated in zeroth order as a single Slater determinant. This Slater determinant serves as a "seed" for improving the wave functions for these nuclei via perturbation theory. Also, the low-lying states for nuclei in between these special cases can be described in eeroth-order by the configurations possible from the valence orbitals.

In many current applications, for all, or a large subset of the nearly degenerate valence configurations, the Hamiltonian can be diagonalized exactly. The spherical shell-model mea" field is used as a basis for evaluating the matrix elements of the residual two-body interaction between the valence particles. The wave functions resulting from such calculations can be used to evaluate various quantities of experimental interest. These quantities range from the energies and J^{π} values which result directly from the Hamiltonian to those which involve expectation values of a few nucleon creation. and annihilation operators. In this way the shell-model wave functions provide a general and complete way of relating a wide variety of nuclear data.

The quality of the wave functions is usually judged first by the comparison of the energies and J^{π} values to experimental data. Then other data on nucleon transfer, electron

Invited talk given by Alex Brow" at the Symposium in Honor of Akito Arima: Nuclear Physics in the 1990's, Santa Fe, May l-5, 1990.

scattering, electromagnetic and beta decay, moments, etc. can be used as a further test of the wave functions. The theoretical input which determines the quality of the wave functions is the completeness of model space and the quality of effective interactions. The use of wave functions which have been successfully tested in this way is important for astrophysical applications and the analysis of fundamental interactions in nuclei such as those involved in isospin nonconservation, parity nonconservation and double-beta decay.

For light nuclei (A<50), one is now able to exactly incorporate most of the configurations within the valence oscillator shells. For these cases the improvements in the wave functions are due to the increase in the number of basis states which can be considered and in the development of better effective Hamiltonians. I will discuss results from these type of calculations. For heavy nuclei, the basis truncation is the main problem and there are many competing models. Intermediate mass nuclei such as those in the A=50-80 region provide a place to compare the more exact approach used for light nuclei with the approximations used in heavier nuclei. This should be a major area of theoretical development in the 1990's.

The computational aspects have been improved by the introduction of more powerful and more general computer codes [3] as well as by the increase in the speed and disk storage capacity of computers. About 15 years ago the full 1s0d-shell matrix for ^{28}Si which has a dimension of about 6,700 in the J-scheme and 94,000 in the M-scheme was considered "state-of-the-art." Within the last few years one can find in the literature calculations which are almost an order of magnitude larger, e.g. about 62,000 in the J-scheme [4], and 320,000 in the M-scheme [5]. With the continued improvement in codes and computers these dimensions could increase another order of magnitude in the 1990's. Overall, however, most of the advance is made possible by the subsequent ability to carry out faster calculations for the smaller dimensions.

Effective interactions continue to be improved. Wildenthal's USD two-body matrix elements for the 1s0d-shell are perhaps the best example of what can be achieved [6]. Analysis of these matrix elements shows that they are qualitatively (about 80%) what is expected from the microscopic G-matrix approach starting from nucleon-nucleon scattering data. However, fine tuning the remaining 20% is essential to obtain good wave functions for all 1s0d-shell nuclei. The reason for this 20% adjustment is not clear, but there are probably many contributing factors. At the level of the G matrix calculation one should make an interpolation of the G matrix elements between ^{16}O and ^{40}Ca. Also one should use radial wave functions which are more realistic than the harmonic oscillator. (This last point opens up the possibility that one should be using single-particle and two-body matrix elements which are much more mass and state dependent than the smooth dependence usually assumed.) In addition, there may be problems beyond the G-matrix level related to modifications of the nucleon properties in the nuclear medium.

Phenomenologically, the effective interaction appears to be well modeled by the effective two-body matrix element form as used by Wildenthal, or the density-dependent potential form used in Hartree-Fock [7] and shell-model [8] applications. The parameters in these forms

should be physically reasonable, and the number of free parameters must be carefully chosen. If the number of parameters is too small, the known data may not be well described. If the number of parameters is too large, the extrapolation is more likely to be incorrect. My current favorite compromise is the "modified surface one-boson exchange potential" (MSOBEP). For the 1s0d-shell, matrix elements obtained from this potential are very similar to Wildenthal's USD matrix elements but has only 17 parameters (compared to Wildenthal's 47). The ^{48}Ca double-beta decay calculations which I will discuss in section 4 are based on a successful application of the MSOBEP to the 1p0f shell [9].

I will illustrate the variety of questions which are being addressed by current shell model calculations in light nuclei by three examples which I put in the form of three questions – Where is the spin? (Section 2), Where are the neutrons? (Section 3), and Where are the neutrinos? (Section 4).

2. WHERE IS THE SPIN?

The form of this question originates from the recent experimental and theoretical investigations related to the spin structure of the nucleon [10]. The issue, of course, is that as of now there no complete theoretical solution to the problem of strongly interacting quarks and gluons in the nucleon, and the answer must rely experimental constraints. The analogous problem of strongly interacting nucleons in the nucleus has largely been solved over the past 40 years by the consistent and large scale application of the shell model. As an example of the progress, I look back at the famous review article on nuclear moments by Noya, Arima and Horie in 1958 [11]. One particular magnetic moment which was poorly understood at the time was that of ^{29}Si (μ_{exp}=−0.555). In the extreme single-particle model, ^{29}Si can be considered as a $1s_{1/2}$ valence neutron outside of a ^{28}Si core formed by the closure of the $0d_{5/2}$ subshell. In this model all of the spin in ^{29}Si is carried by the intrinsic spin of the valence neutron and the single-particle magnetic moment is $\mu_{1s_{1/2}}$=−1.91. In addition to this simple valence configuration, Noya, Arima and Horie considered the first-order correction arising from the $0d_{5/2}^{-1}$-$0d_{3/2}$ excitation of the core. They obtained improved agreement with the experimental magnetic moment but were still a factor of two off ($\mu_{1s_{1/2}} + \delta\mu$=−1.02). The value of μ_{1s0d}=−0.502 obtained with Wildenthal's interaction in the full 1s0d shell model basis is in much better agreement with experiment.

It is interesting to compare the expectation value of J_z in ^{29}Si obtained in the extreme single-particle model to that obtained from the full 1s0d-shell wave functions. This comparison is made in Table 1. In the full basis only about half of the total spin is carried by the intrinsic spin of the valence neutron. (One might naively think that this reduction is closely related to the reduction in the $1s_{1/2}$ orbit occupancy. However, it turns out the occupation of the $1s_{1/2}$ orbit in the full 1s0d-shell basis is actually about 10% larger than in the extreme single-particle model.) Most of the spin turns out to reside in the orbital motion of the neutron. (This is qualitatively as expected in the first-order calculation of Noya, Arima and Horie.)

Table 1: J_z expectation values in ^{29}Si

Particle	Type	ℓ	Extreme Single Particle Model	Full 1s0d Model
neutron	spin	s	+ 0.5	+ 0.282
	spin	d	0	− 0.148
	orbital	d	0	+ 0.350
proton	spin	s	0	+ 0.005
	spin	d	0	− 0.007
	orbital	d	0	+ 0.018
total			+ 0.5	+ 0.5

One has confidence in these predictions of the spin distribution not just from the magnetic moment ^{29}Si, but also because the magnetic moments calculated with Wildenthal's interaction throughout the 1s0d-shell are in excellent agreement with experiment. This is illustrated in Fig. 1. On the left-hand side all known magnetic moments in the 1s0d-shell are compared with those obtained in the extreme single-particle model. On the right-hand side the same data are compared with the full 1s0d-shell model (using free-nucleon g factors). The difference is dramatic. Experimental (e,e') data on the elastic magnetic form factor of ^{29}Si provides a further means to test the calculations [12].

Of course the 1s0d-shell basis by itself is not a complete description of these nuclei. There are admixtures from higher shells as well as non-nucleonic degrees of freedom to consider. Arima and his coworkers have played a major role in understanding these [13]. Within the 1s0d-shell basis it is possible to improve the agreement between experiment and theory further by using effective operators which take into account in some average way these higher order effects [14]. This is illustrated in Fig. 2. On the left-hand side the experimental magnetic moments are compared with the ones calculated in the full 1s0d-shell basis using free-nucleon operators (the same as the right-hand side of Fig. 1). On the right-hand side the same data are compared with the magnetic moments calculated with the effective operator. There are many interesting conclusions one can draw [14] from a comparison of the empirical effective operators for Gamow-Teller and M1 matrix elements with those calculated [13,15]. I will mention only one here – namely that the well-known quenching observed in the Gamow-Teller transitions can be attributed mostly (about 65%) to higher-order nuclear configuration mixing and only

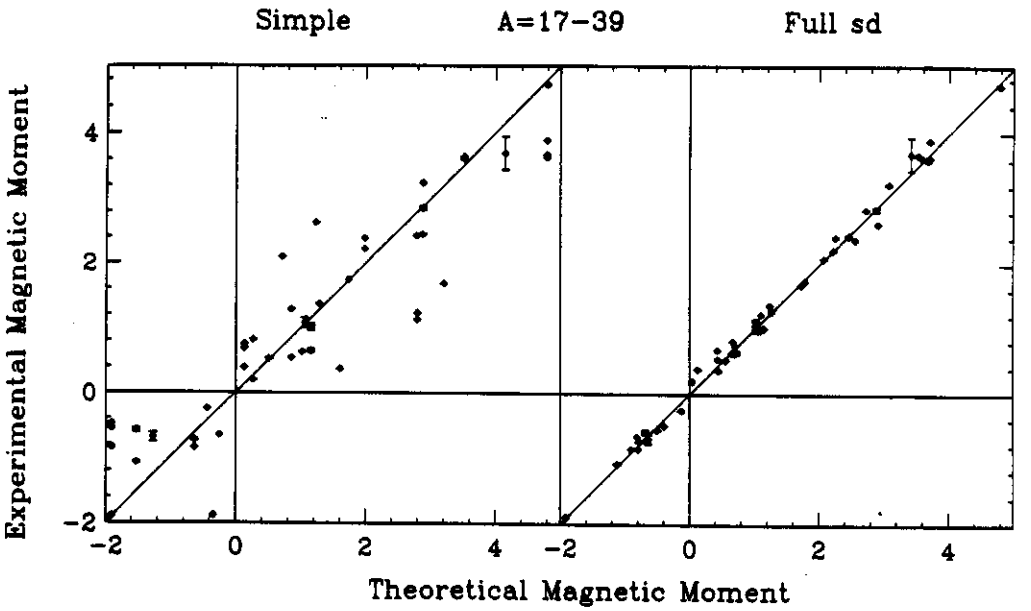

Figure 1: Comparison of experimental (y) and theoretical (x) magnetic moments for 1s0d-shell nuclei. The theoretical values for the right-hand side were obtained with the full 1s0d-shell basis, and those on the left-hand side were obtained with only the largest component in the wave function (corresponding to the extreme single-particle model). Free nucleon g-factors are used in both cases.

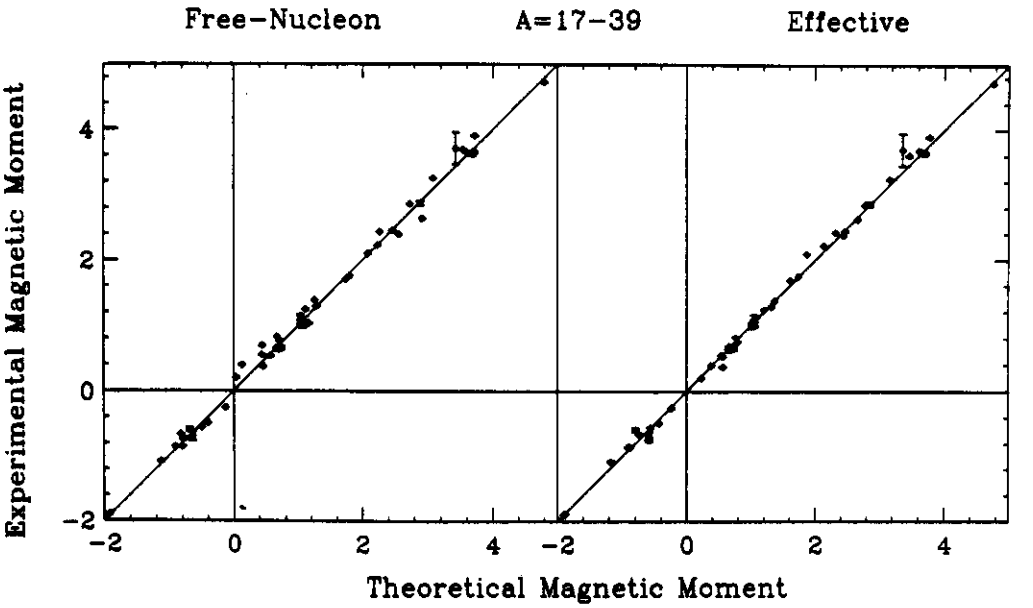

Figure 2: Comparison of experimental (y) and theoretical (x) magnetic moments for 1s0d-shell nuclei. The theoretical values for both sides were obtained with the full 1s0d-shell basis. The theoretical values left-hand side were obtained using free-nucleon g-factors, and those on the right-hand side were obtained using effective g-factors.

partly (about 35%) to the non-nucleonic degrees of freedom involving the delta resonance.

3. WHERE ARE THE NEUTRONS?

Our knowledge of light nuclei is rapidly being pushed out to the neutron and proton drip lines by recent and planned experiments. Some of the most interesting results are obtained for those nuclei near neutron drip line where the neutron to proton ratio is close about two to one. It is a challenge for nuclear models to extrapolate out to these nuclei. There are several particularly interesting problems related to the shell model orbits and configurations which the valence neutrons occupy in these nuclei.

Many properties of the isotones with N=20 neutrons and Z=8-20 protons are now known. The nuclei with Z>13 have binding energies and spectra which are as expected from Wildenthal's 1s0d-shell wave functions. One example is the recently studies case ^{34}Si [16]. However, it is well known that there is a region of nuclei centered around ^{32}Mg which has binding energies, spectra and decay properties which are very different than that expected in the 1s0d model space [17,18]. This is illustrated by the differences between experimental and theoretical binding energies shown in Fig. 3.

An extensive new set of shell-model calculations has recently been carried out for these nuclei which include both the 1s0d and 1p0f shells [19]. These calculations make use of the Warburton-Becker-Millener-Brown (WBMB) Hamiltonian which is based on single-particle energies and interactions adjusted to reproduce the properties of nuclei near ^{40}Ca [20]. All initial calculations were carried out under the assumption that the nucleons occupy the lowest available oscillator shell. These calculations provide a reasonable account of experimental data in the region $19 \leq N \leq 24$ and $14 \leq Z \leq 20$ [21]. However, when they are extended below Z=14 there are discrepancies with the experimental binding energies for N>20 which continue the trend previously observed with Wildenthal's USD interaction at N=20. The comparison shown in Fig. 3 for N>20 is based on these WBMB calculations.

We have investigated this problem by carrying out more extended calculations in which two nucleons are allowed to be excited from the 1s0d shell to the 1p0f shell. We will refer to these as 2p-2h or $2\hbar\omega$ configurations. It turns out that neutron excitations are far more important than proton excitations for these neutron-rich nuclei [19]. Also, for the reasons discussed in Ref 19, we do not allow mixing between the $0\hbar\omega$ and $2\hbar\omega$ configurations. In general, the dimensions associated with these $2\hbar\omega$ configurations are too large to easily handle (greater than about 10,000). However, the $2\hbar\omega$ calculations were possible for nuclei near ^{28}O and ^{40}Ca. In the case of ^{30}Ne we found that the binding energy of the $2\hbar\omega$ configuration turned out to be about one MeV greater than that of the $0\hbar\omega$ configuration. From a comparison of such calculations for ^{28}O, ^{30}Ne, ^{38}Ar and ^{40}Ca we found that the relative binding energies of the $2\hbar\omega$ and $0\hbar\omega$ configurations in ^{30}Ne could be qualitatively understood as a sum of three contributions – (1) a 10 MeV decrease due to the 1s0d-1p0f single-particle gap of about 5 MeV, (2) a 7 MeV increase due to the proton-neutron interaction between the two 1s0d-shell

protons and the two 1p0f-shell neutrons, and (3) a 4 MeV increase in the neutron-neutron "pairing" interaction due to promotion of two neutrons from the closed 1s0d-shell to the open 1p0f shell.

Furthermore, this analysis revealed that the energy of the $2\hbar\omega$ configuration is well approximated by a weak-coupling model similar to the one used to estimate the energies of multi-particle multi-hole states in ^{16}O and neighboring nuclei [22]. For example, the excitation energy of the $2\hbar\omega$ configuration in ^{30}Ne relative to the $0\hbar\omega$ configuration is given by Ex = $-$BE(^{28}Ne)$-$BE(^{32}Ne)+ 2xBE(^{30}Ne)$-$4C, where BE are the binding energies of $0\hbar\omega$ configurations and C is the average particle-hole interaction between the two neutron-holes in the 1s0d shell and the two neutron-particles in the 1p0f shell. From a comparison of the exact and weak-coupling energies we obtain C = 250 keV. Since it is possible to carry out essentially all of the needed $0\hbar\omega$ calculations, we are able to use this type of weak-coupling expression to estimate the excitation energies of the $2\hbar\omega$ configurations (as well as the energies of all $n\hbar\omega$ configurations) in all nuclei of interest. From these estimates we find an "island of inversion" extending from N=20-22 and Z=10-12 where the $2\hbar\omega$ configuration is predicted to be the ground state (see Fig. 4). Recent improvements in the mass measurement for these nuclei [23] seem to confirm our predictions. Low-lying $1\hbar\omega$ states in the N=19 and N=21 isotones with Z=9-14 are related to the same phenomena [19] and are also seen experimentally [24]. The extent of this island as a function of Z is controlled by the Z-dependence in the proton-neutron interaction between the 1s0d-shell protons and the 1p0f-shell neutrons. The Z dependence arises from the varying collectiveness of the 1s0d-shell proton configuration. It is the semi-closed shell nature of the proton configuration in ^{34}Si (Z=14) [16] that is responsible for the disappearance of the island of inversion for Z>12.

A similar pattern with intruder states arises for the nuclei near ^{12}Be. The most obvious indication of this is the well known $1/2^+$ $1\hbar\omega$ ground state of ^{11}Be. The existence of low-lying $2\hbar\omega$ configurations in ^{12}Be or neighboring nuclei has not been established experimentally. The lowering of the $1/2^+$ configuration in this mass region as been related to the lowering of the $1s_{1/2}$ single-particle state in the finite potential well [25]. However, prolate deformation is probably the simplest qualitative way to understand these intruder states in both the 0p-1s0d and 1s0d-1p0f regions. In both cases the intruder Nillson orbital with k=1/2 drops in energy very sharply as a function of deformation.

In this mass region, ^{11}Li has recently received the most attention. In this nucleus on the neutron-drip line is unusual because the two-neutron separation energy is exceptionally small, S_{2n}=$-$0.19(11) MeV, compared to the one-neutron separation energy, S_n=$-$1.0(3) MeV. In spite of this, the spin (J^π=3/2$^-$), magnetic moment (μ_{exp}=3.667) [26] and half-life [27] are in reasonable agreement with the p-shell calculation of these quantities (J^π=3/2$^-$ and $\mu_{0\hbar\omega}$=3.793). A comparison with the magnetic moment of $\mu_{2\hbar\omega}$=2.997 obtained with a pure $2\hbar\omega$ configuration indicates that the $2\hbar\omega$ of intruder state is not the dominant component of the ground

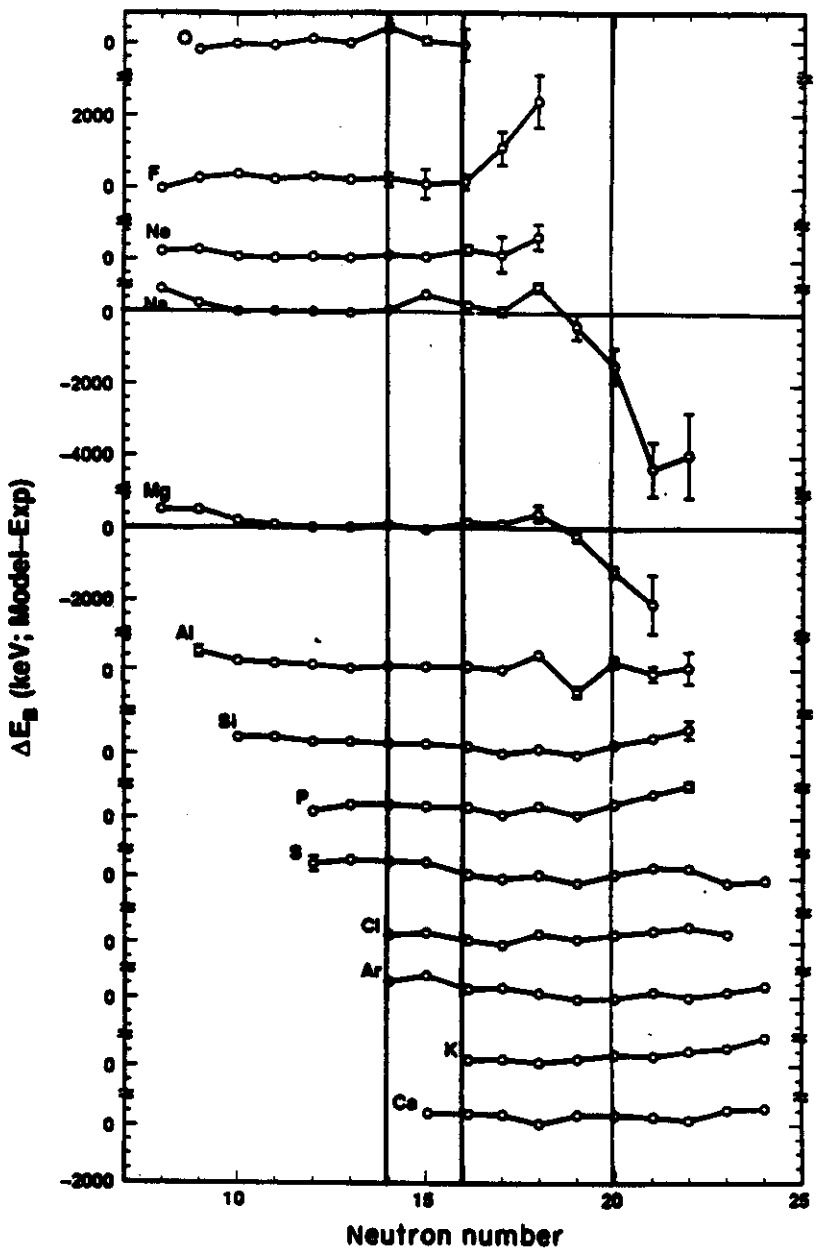

Figure 3: Differences between the measured and calculated binding energies for the neutron-rich 1s0d-1p0f region. The calculations are based on Wildenthal's USD interaction for N$\leq$20 and on the WBMB interaction for N>20. The lines indicate the semi-magic numbers N=14 and N=16 and the zero for the Na and Mg isotope differences.

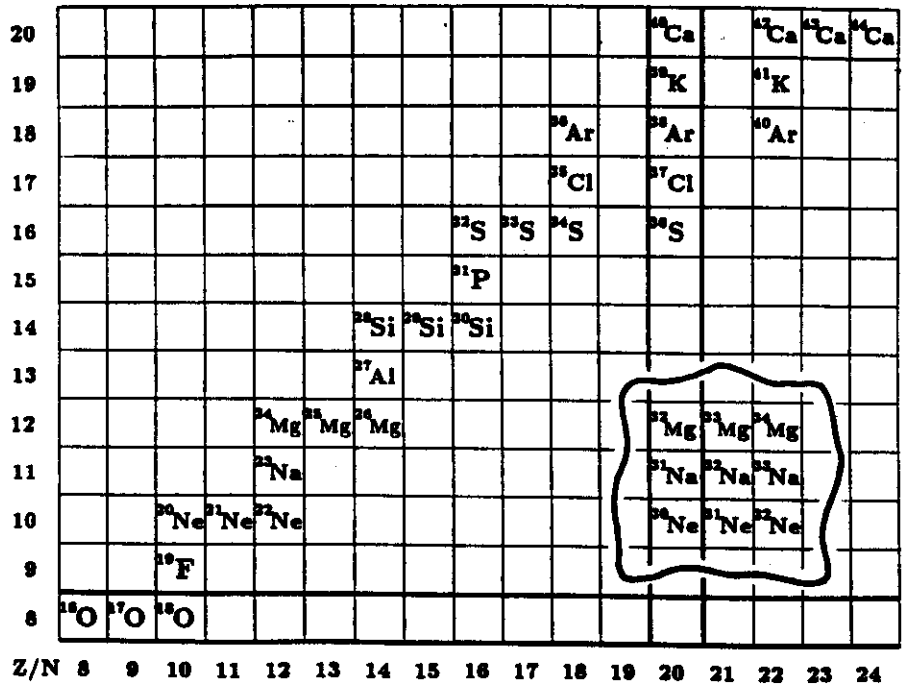

Figure 4: Partial periodic table highlighting the "island of inversion" centered at ^{32}Na. The magic numbers Z=8 and N=20 are emphasized with double lines. Apart from the "island" only stable nuclei are shown.

state.

Hoshino, Sagawa and Arima (HSA) [28] have recently carried out $2\hbar\omega$ calculations for ^{11}Li. They are similar to the WBMB calculations described above for the 1s0d-1p0f shell except that HSA allow for mixing between the $0\hbar\omega$ and $2\hbar\omega$ configurations and WBMB do not. HSA obtain a very small admixture of $2\hbar\omega$ into the predominantly $0\hbar\omega$ ^{11}Li ground state. However, we have shown that allowing for mixing between the $0\hbar\omega$ and $2\hbar\omega$ configurations results in an underestimation of the admixture [19]. In the following discussion I will assume a 0p-shell configuration for ^{11}Li.

A dramatic property of ^{11}Li is the relatively large cross section observed in the high-energy scattering of a secondary beam of ^{11}Li from stable nuclei [29]. For the scattering of ^{11}Li on light nuclei where the cross section must be dominated by the nuclear interaction, the large cross sections are qualitatively associated with a relatively large matter radius. The experimental cross sections for ^{11}Li and neighboring nuclei are well reproduced by Glauber-type calculations based on nuclear matter densities obtained from our constrained spherical Hartree-Fock calculations [30]. Since Hartree-Fock calculations even for the stable nuclei usually do not reproduce the single-particle energies to better than a few MeV, it is important to constrain the depth of the potential to reproduce the experimental separation energies of the valence neutron [30].

In Fig. 5 I show that proton and neutron density distributions for ^{11}Li obtained from these constrained Hartree-Fock calculations. The long tail corresponds the Hankel functions of a

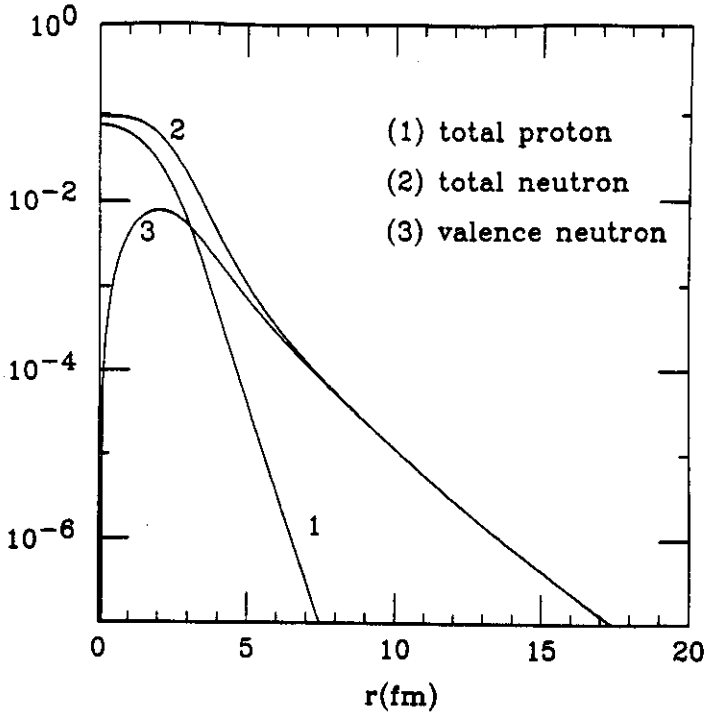

Figure 5: Proton and neutron density distributions for ^{11}Li obtained from the constrained Hartree-Fock calculations.

$0p_{1/2}$ neutron bound by 1 MeV. First, I note that the present high-energy scattering experiments are not sensitive to the density beyond about 6 fm. Second, I note that the calculation is in the mean-field approximation and does not take into account the possible correlations between the two loosely bound valence neutrons. In the extreme dineutron cluster model for the two-neutrons one might imagine that the tail should fall off with a slope characteristic of the two-neutron separation energy, that is about 200 keV. Clearly it is important to have better experiments for the ^{11}Li mass and experiments such as sub-Coulomb scattering which would be more sensitive to the density distribution in the tail.

Perhaps the most interesting property of ^{11}Li is the large Coulomb excitation cross section observed scattering of a secondary beam of ^{11}Li from ^{208}Pb [31]. This large cross section indicates that there must be significant dipole strength at very low excitation energy. Conventional nuclear structure calculations, even those that include $3\hbar\omega$ excitations [32], cannot reproduce enough dipole strength at low energy. However, a recent continuum RPA calculation appears to be in better agreement with experiment [33]. Also the dipole strength can be understood in the extreme dineutron cluster model [34] (although with a large uncertainty due to the experimental error in the two-neutron separation energy.) A consistent model for ^{11}Li and the neighboring nuclei must also explain the momentum distributions of the fragments [35]. The experimental and theoretical study of ^{11}Li and other nuclei on the neutron and proton drip

lines will remain a challenge for the 1990's.

4. WHERE ARE THE NEUTRINOS?

The study of double-beta decay in nuclei is an area where nuclear physics can add to the understanding of fundamental particles and interactions. Standard two-neutrino double-beta ($2\nu\beta\beta$) decay is a process which should proceed as expected from the second-order weak interaction process. The first laboratory observation of $2\nu\beta\beta$ has recently been reported [36]. Nonstandard zero-neutrino double-beta ($0\nu\beta\beta$) decay is allowed only if the neutrino has a mass; it also depends on the form of the weak interaction currents [37,38]. As of now there are only experimental limits on $0\nu\beta\beta$ decay.

It turns out that the nuclear matrix elements for $\beta\beta$ are very hindered relative to the single-particle estimates and are thus sensitive to nuclear structure considerations. In fact most of the nuclei of interest are in the A=76-100 mass range where the type of large-scale shell-model calculations I have been discussing are very difficult. The most reliable results to date for these nuclei are thought to be obtained from QRPA calculations [39,40,41]. When these QRPA calculations are compared to the experimental limits which exist on $0\nu\beta\beta$ decay, the upper limits on the neutrino mass are in a range of less 2-10 eV [39]. Further improvements in the experimental limits may be able to push this limit down to the range of a few tenth of keV. This is also consistent with the 27 eV upper limit obtained in the Los Alamos tritium decay experiment (Ref 42, although inconsistent with the Russian result [43]. Even though there is only an outside chance that the neutrino mass is in the range of 0.1 to 10 keV, it is important to continue to improve the experimental and theoretical analysis.

Here I want to discuss some new calculations for the $\beta\beta$ decay of ^{48}Ca carried out by Liang Zhao and myself [44]. Although ^{48}Ca has the largest $\beta\beta$ Q-value [37], it has not been as well studied as some of the heavier nuclei. Experimentally this is because the ^{48}Ca source is not easy to obtain or handle. Theoretically the $\beta\beta$ matrix elements are thought to be particularly hindered. However, ^{48}Ca is interesting because it can be calculated in a much more complete basis than is possible for the heavier nuclei.

We have calculated the $2\nu\beta\beta$ decay in much larger model space than previously used and with a new interaction which we test by comparing with the β^+ and β^- spectra obtained from recent ^{48}Ti(n,p) and ^{48}Ca(p,n) experiments. In previous calculations where the intermediate 1^+ states have been considered explicitly, the 1p0f shell model space was highly truncated [45,46,47], and in other cases where the truncation was not so severe, the closure approximation was used [37,48]. Most recently, Horie and Ogawa carried out the $2\nu\beta\beta$ in the full 1p0f model space but with a new method that does not require an explicit spectrum of intermediate 1^+ states [49].

Our calculations were carried out in the truncation defined by $0f_{7/2}^{8-r}(1p_{3/2},0f_{5/2},1p_{1/2})^r$ where $r\leq 4$ for the 0^+ ground states of ^{48}Ca and ^{48}Ti and $r\leq 5$ for the 1^+ states in ^{48}Sc. In this truncation there are 5599 1^+, T=3 states in ^{48}Sc. The $2\nu\beta\beta$ matrix element obtained

in this truncation is within a few percent of the one obtained by Horie and Ogawa [49] in the full 1p0f model space ($r \leq 8$) with the same interaction. Additional comparisons of truncated and full space calculations for the $2\nu\beta\beta$ matrix element for ^{46}Ca and 1s0d-shell nuclei, lead us to conclude that our truncation gives results for the ^{48}Ca $\beta\beta$ decay which are essentially the same as those that would be obtained in the full 1p0f model space.

We have compared the results obtained with two interactions. One (which we label by MH) used by Tsuboi, Muto and Horie in a very truncated calculation ($r \leq 2$) [45] and then by Horie and Ogawa in the full space calculation [49]. The MH interaction has a long history. McGrory et al. [50] started with the renormalized Kuo-Brown interaction and changed several T=1 two-body matrix elements which involved the $0f_{7/2}$ and/or $1p_{3/2}$ orbits. Later McGrory et al. [51] added 50 keV to the $0f_{7/2}$-$0f_{5/2}$ diagonal T=1 matrix elements and introduced new single-particle energies. Based on Ref 50, Muto and Horie [52] shifted the monopole part of the inter-shell T=0 matrix elements $<0f_{7/2},j|V|0f_{7/2},j>$ ($j=1p_{3/2},1p_{1/2},0f_{5/2}$) by -0.3 MeV.

Our new interaction labeled MSOBEP is based on the modified surface one-boson exchange potential [8]. Parameters of this potential have been determined by a fit to 61 energy level and binding energy data for nuclei in the lower part ($A<48$) of the 1p0f shell [9]. The parameters varied were six strengths associated with the central part of the potential and the four single-particle energies. The parameters associated with the spin-orbit and tensor parts of the potential were kept fixed at the values obtained in the 1s0d shell [8]. The rms deviation between experiment and theory was 176 keV.

The effects of higher-order configuration mixing outside the 1p0f shell and mesonic exchange currents (including Δ-isobar nucleon-hole configurations) were taken into account by using the effective Gamow-Teller operator given by $\sigma t^-(\mathrm{eff}) = 0.77\sigma t^-$. This renormalized form of the effective operator is empirically well established from beta decay data in the 1s0d shell [53] and 1p0f shell [54,55]. Also, the contributions of these effects to the interaction are presumably taken into account by the adjustments of the potential parameters to fit experimental binding energies. The direct contribution of the Δ-isobar nucleon-hole configurations on the $\beta\beta$ decay is negligible because of the large energy denominator and because of cancellations between β^+ and β^- [48,56]. We believe that the direct contribution of the higher-order configuration mixing on the $\beta\beta$ matrix element is small, but should be further investigated.

We write the $2\nu\beta\beta$ matrix element as

$$M_{GT}(E_m) = \Sigma_{m=1}^{E_m} <0_f^+ \,||\, \sigma t^-(\mathrm{eff})||1_m^+ > <1_m^+ \,||\, \sigma t^-(\mathrm{eff})||0_i^+ > / \,(E_m+E_o)$$

where $E_o = (T_o/2)+\Delta M$, T_o is the $\beta\beta$ Q-value (4.27 MeV), ΔM is the mass difference between ^{48}Sc and ^{48}Ca (-0.277 MeV), and E_m is the excitation energy of the 1_m^+ state in ^{48}Sc. The total $2\nu\beta\beta$ matrix element is given by $M_{GT}^{2\nu}=M_{GT}(E_m=\infty)$. The Fermi contribution vanishes when isospin is conserved and an estimate of its contribution with isospin-mixed wave functions

indicates that it can be neglected [46]. The half-life is given by

$$(1/T_{1/2}) = G\ |M^{2\nu}_{GT}\ |^2$$

where G is related to the fundamental constants and phase space integrals which depend somewhat on the intermediate state strength distribution [45]. We use a value of G=1.10x10^{-17} yr^{-1} (MeV)^2 deduced from the first row in Table 1 of Ref 45.

The individual matrix in the expression for M^m_{GT} can be studied with in the ^{48}Ti(n,p) and ^{48}Ca(p,n) reactions. In Fig. 6 I show the B(GT$^-$) = $|<1^+_m\ ||\ \sigma t^-(\mathrm{eff})||0^+_i>|^2$ values for the ^{48}Ca to ^{48}Sc transitions as a function of excitation energy. Since there are several hundred 1^+ states calculated to be in the region between 5 and 15 MeV excitation, the B(GT) values have been smoothed over a Gaussian function. The bottom curve is the GT distribution extracted from the peaks above the background in the experimental cross section at 0^o [54]. The middle spectra show the calculations for the GT distribution for the MH (dotted curve) and MSOBEP (solid curve) interactions with a full width at half maximum (FWHM) of 400 KeV chosen to match the experimental resolution. (The top curve shows the MSOBEP results with 100 keV FWHM to show what the ideal experiment might look like.) The results with the MSOBEP interaction are in best agreement with experiment. The apparent overestimation of strength in the region around 10 MeV in excitation energy is resolved by including the extra strength extracted from the background spectrum. It is interesting to note that the lowest 1^+ state obtained with the MH interaction does not have the predominant $(\nu 0f_{7/2})^{-1}(\pi 0f_{7/2})^1$ structure expected from experiment. Rather, this interaction pulls down another configuration which appears to have a ^{48}Ca + deuteron cluster structure as its dominant configuration. Thus the "particle-particle" part of the MH interaction appears to be slightly too strong.

In Fig. 7 I show the B(GT$^+$)=$|<0^+_f\ ||\ \sigma t^-(\mathrm{eff})||1^+_m>|^2$ values for the ^{48}Ti to ^{48}Sc transitions as a function of excitation energy. In this case each B(GT) value is shown by an isolated peak. The bottom curve shows the values deduced by a fit of the experimental (n,p) spectrum [57] to peaks centered at the known location of 1^+ states. Comparison with the calculations again shows that the MSOBEP results (middle spectrum) are in better agreement with experiment than the MH results (top spectrum).

These comparisons show the importance of being able to explicitly calculate the spectra of the intermediate 1^+ states and the importance of having experimental data for both the β^- and β^+ directions. The individual β^+ and β^- matrix elements can now be combined to form the $2\nu\beta\beta$ matrix element. In Fig. 8 I show $M_{GT}(E_m)$ as a function of E_m for the MH (dotted line) and MSOBEP (solid line) interactions. The general feature of these curves is similar to what has been found in an earlier more truncated calculation [45], namely, a quick rise from the first few states, followed by a more gradual rise from the states up to about 6 MeV in excitation, followed by a fall off (cancellation) from the remaining states up to about 10 MeV in excitation. The qualitative nuclear structure reasons for this pattern is discussed in [46,44]. It is remarkable that the total matrix element in the MSOBEP calculation (0.070) is

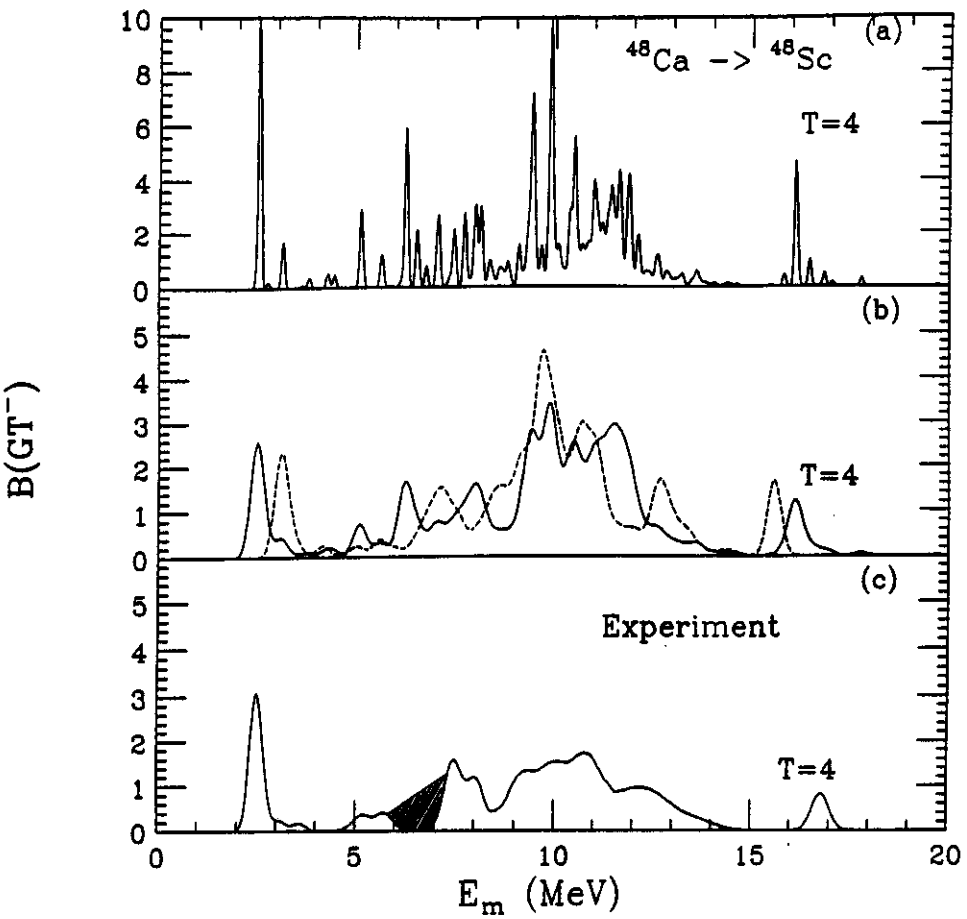

Figure 6: B(GT$^-$) values for ^{48}Ca to ^{48}Sc as a function of E_m. The bottom curve is the GT distribution extracted from the peaks above the background in the experimental (p,n) cross section at 0° [54]. The shaded area indicates the region where the Fermi transition to the 0^+ state has been subtracted. The theoretical curves are obtained by averaging the B(GT) values for individual states over a Gaussian distribution. The middle spectra for the MH (dashed line) and MSOBEP (solid line) interactions were obtained with FWHM=400keV. The top spectrum for the MSOBEP interaction was obtained with FWHM=100keV.

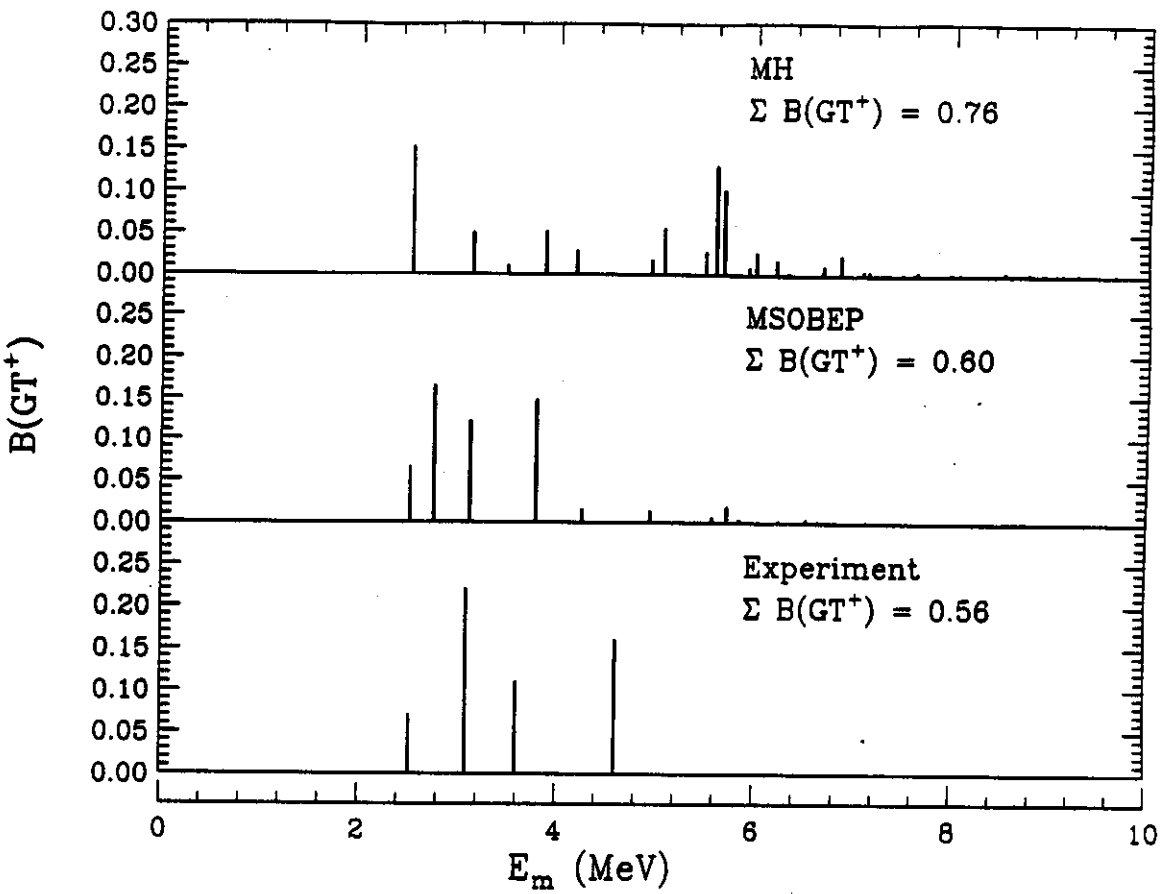

Figure 7: $B(GT^+)$ values for ^{48}Ti to ^{48}Sc as a function of E_m. Each B(GT) value is indicated by an isolated peak. The bottom curve shows the values deduced by a fit of the experimental (n,p) spectrum [57] to peaks centered at the known location of 1^+ states.

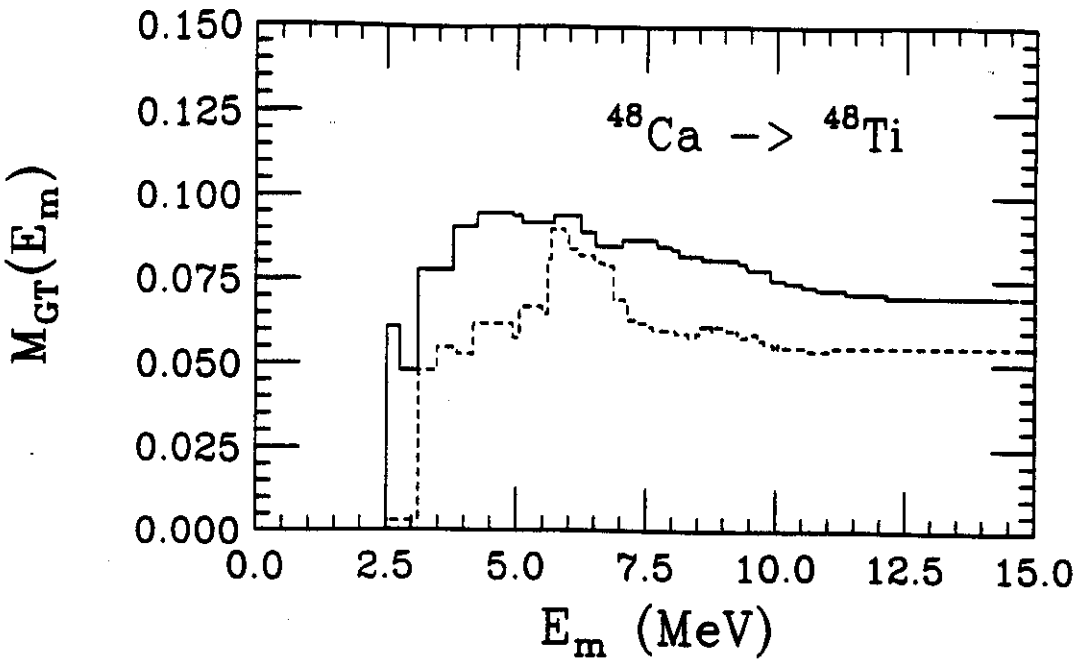

Figure 8: The $2\nu\beta\beta$ matrix element $M_{GT}(E_m)$ as a function of E_m. The solid line corresponds to the results with the MSOBEP interaction and the dashed line corresponds to those for the MH interaction.

very close to the contribution from the first state alone (0.061).

The value of $M_{GT}^{2\nu}$=0.070 $(MeV)^{-1}$ obtained with the MSOBEP interaction translates into a $2\nu\beta\beta$ $T_{1/2}$ value of $1.9\text{x}10^{19}$yr compared to the experimental lower limit of $>3.6\text{x}10^{19}$yr [58]. This disagreement between theory and experiment is a puzzle – and the source of the question – where are the neutrinos? It turns out that the MH interaction gives a result of $3.0\text{x}10^{19}$yr which is in better agreement with experiment. However, we have shown above that the MH interaction does not reproduce the β^- and β^+ spectra. It may be that the $2\nu\beta\beta$ matrix element is sensitive to further refinements in the interaction and to the direct effects of the higher-order configuration mixing which do not show up in the β^- and β^+ comparisons made above. In particular, we note that there is a large uncertainty in the Gamow-Teller strength extracted from the (n,p) spectrum above 5 MeV in excitation energy [57]. In any case, it is remarkable that the best calculations and the experimental limit agree with each other within a factor of two out of many possible orders of magnitude, and we hope to encourage further experimental efforts on the ^{48}Ca decay. Calculations for the $0\nu\beta\beta$ matrix elements are in progress. An estimate from previous calculations [46] compared to the experimental lower limit of $T_{1/2}(0\nu\beta\beta)>200\text{x}10^{19}$yr [58] gives an upper limit of about 20 eV for the neutrino mass. The $0\nu\beta\beta$ matrix element for ^{48}Ca turns out to be less sensitive to the truncation that the $2\nu\beta\beta$ matrix element [46]. Continued theoretical and experimental investigations of double-beta decay in nuclei will be a important application of nuclear physics in the 1990's.

5. POSTSCRIPT

Clearly there are many interesting problems to consider and applications to make in the area of nuclear physics in the 1990's. So to conclude, let me quote a famous Haiku of Basho [59] – "Furuike ya, kawazu tobikomu, mizu no oto" – which for the purpose of this meeting I will translate as – "nuclear physics is an old subject, but we should jump in and make a splash."

ACKNOWLEDGEMENT

This work was supported in part by the US National Science Foundation grant number PHY-87-14432.

REFERENCES

1. B. A. Brown, in The Nuclear Shell Model, edited by T. -S. H. Lee and R. B. Wiringa, (North Holland, Amsterdam, 1990).
2. B. A. Brown and B. H. Wildenthal, Ann. Rev. of Nucl. and Part. Sci. 38 (1988) 29.
3. B. A. Brown, in Workshop on Microscopic Models in Nuclear Structure Physics, edited by M. W. Guidry, J. H. Hamilton, D. H. Feng, N. R. Johnson and J. B. McGrory (World Scientific, singapore, 1989) p. 337.
4. K. Ogawa and H. Horie, in Nuclear Weak Process and Nuclear Structure, edited by M. Morita, H. Ejiri, H. Ohtsubo and T. Sato, (World Scientific, Singapore, 1989) p. 308.
5. J. A. Carr et al., Phys. Rev. Lett. 62 (1989) 2249.
6. B. H. Wildenthal, Progress in Particle and Nuclear Physics 11 (1984) 5.
7. J. Decharge and D. Gogny, Phys. Rev. C33 (1986) 335.
8. B. A. Brown, W. A. Richter, R. E. Julies and B. H. Wildenthal, Ann. Phys. 182 (1988) 191.
9. W. A. Richter, R. E. Julies and B. A. Brown, unpublished.
10. H. J. Lipkin, Phys. Lett. 237B (1990) 130.
11. H. Noya, A. Arima and H. Horie, Prog. Theor. Phys. Suppl. 8 (1958) 33.
12. B. A. Brown, R. Radhi and B. H. Wildenthal, Phys. Lett. 133B (1983) 5.
13. A. Arima et al., Adv. Nucl. Phys. 18 (1987) 1.
14. B. A. Brown and B. H. Wildenthal, Nucl. Phys. A474 (1987) 290.
15. I. S. Towner, Phys. Reports 155 (1987) 263.
16. P. Baumann et al., Phys. Lett. 228B (1989) 458.
17. X. Campi et al., Nucl. Phys. A251 (1975) 193.
18. B. H. Wildenthal, M. S. Curtin and B. A. Brown, Phys. Rev. C28 (1983) 1343.

19. E. K. Warburton, J. A. Becker and B. A. Brown, Phys. Rev. C41 (1990) 1147.

20. E. K. Warburton, J. A. Becker, D. J. Millener and B. A. Brown, BNL Report 40890 (1987); Ann. Phys. 187 (1988) 471.

21. E. K. Warburton et al., Phys. Rev. C34 (1986) 1031; J. W. Olness et al., Phys. Rev. C34 (1986) 2049; E. K. Warburton, Phys. Rev. C35 (1987) 2278; E. K. Warburton and J. A. Becker, Phys. Rev. C35 (1987) 1851; Phys. Rev. C37 (1988) 754; Phys. Rev. C39 (1989) 1535; Phys. Rev. C40 (1989) 2823.

22. L. Zamick, Phys. Lett. 19 (1965) 580; R. D. Lawson, Theory of the Nuclear Shell Model, (Clarendon Press, Oxford, 1980).

23. N. A. Orr et al., (GANIL collaboration) unpublished.

24. P. Baumann et al., unpublished.

25. I. Talmi and I. Unna, Phys. Rev. Lett. 4 (1960) 496.

26. E. Arnold et al., Phys. Lett. 197B (1987) 311.

27. M. S. Curtin et al., Phys. Rev. Lett. 56 (1986) 34.

28. T. Hoshino, H. Sagawa and A. Arima, Nucl. Phys. A506 (1990) 271.

29. I. Tanihata et al., Phys. Rev. Lett. 55 (1985) 2676; Phys. Lett. 160B (1985) 380.

30. G. F. Bertsch, B. A. Brown and H. Sagawa, Phys. Rev. C39 (1989) 1154.

31. T. Kobayashi et al., Phys. Lett. 232B (1989) 497.

32. T. Hoshino, H. Sagawa and A. Arima, to be published.

33. G. Bertsch and J. Foxwell, Phys. Rev. C41 (1990) 1300 and errata, to be published, which gives the corrected values for the Coulomb excitation cross section for 800 MeV/nucleon ^{11}Li on ^{208}Pb as 0.25 to 0.7 bn.

34. P. G. Hansen and B. Jonson, Europhys. Lett. 4 (1987) 409.

35. T. Kobayashi et al., Phys. Rev. Lett. 60 (1988) 2599.

36. S. R. Elliott, A. A. Hahn and M. K. Moe, Phys. Rev. Lett. 59 (1987) 2020.

37. W. C. Haxton and G. J. Stephenson, Prog. in Part. and Nucl. Phys. 12 (1984) 409.

38. M. Doi et al., Prog. Theor. Phys. Suppl. 83 (1985) 1.

39. K. Muto, E. Bender and H. V. Klapdor, Z. Phys. 334 (1989) 177; 334 (1989) 187.

40. T. Tomoda and A. Faessler, Phys. Lett. 199B (1987) 475.

41. J. Engel, P. Vogel and M. R. Zirnbauer, Phys. Rev. C37 (1988) 731.

42. J. F. Wilkerson et al., Phys. Rev. Lett. 58 (1987) 2023.

43. S. Boris et al., Phys. Rev. Lett. 58 (1987) 2019.

44. L. Zhao and B. A. Brown, Phys. Rev. C, to be published.

45. T. Tsuboi, K. Muto and H. Horie, Phys. Lett. 143B (1984) 293.

46. B. A. Brown, in Nuclear Shell Models, edited by M. Vallieres, and B. H. Wildenthal, (World Scientific, Singapore, 1985), p. 42.

47. L. D. Skouras and J. D. Vergados, Phys. Rev. C28 (1983) 2122; J. D. Vergados, Phys. Rep. 133 (1986) 1.

48. L. Zamick and N. Auerbach, Phys. Rev. C26 (1982) 2185.

49. K. Ogawa and H. Horie, in Nuclear Weak Process and Nuclear Structure, edited by M. Morita, H. Ejiri, H. Ohtsubo and T. Sato, (World Scientific, Singapore, 1989), p. 308.

50. J. B. McGrory, B. H. Wildenthal and E. C. Halbert, Phys. Rev. C2 (1970) 186.

51. J. B. McGrory and B. H. Wildenthal, Phys. Lett. 103B (1981) 173.

52. K. Muto and H. Horie, Phys. Lett. 138B (1984) 9.

53. B. A. Brown and B. H. Wildenthal, At. Data and Nucl. Data Tables 33 (1985) 347.

54. B. D. Anderson et al. Phys. Rev. C31 (1985) 1161, and private communication.

55. J. Rapaport et al., Nucl. Phys. A427 (1984) 332.

56. K. Grotz and H. V. Klapdor, Nucl. Phys. A460 (1986) 395.

57. W. P. Alford et al., to be published in Nucl. Phys. A.

58. R. K. Bardin et al., Nucl. Phys. A158 (1970) 337.

59. R. H. Blyth, Haiku Vol. 1 (Hokuseido Press, Tokyo, 1949), p. 277. (The more correct translation is: The old pond, A frog jumps in, The sound of water.)